Available online at www.sciencedirect.com
SCIENCE DIRECT®
Applied Catalysis B: Environmental 60 (2005) 231–240
APPLIED CATALYSIS B: ENVIRONMENTAL
www.elsevier.com/locate/apcatb

Effects of zeolite structure and aluminum content on thiophene adsorption, desorption, and surface reactions

Antonio Chica [a], Karl G. Strohmaier [b], Enrique Iglesia [a,*]

[a] *Department of Chemical Engineering, University of California at Berkeley, Berkeley, CA 94720, USA*
[b] *ExxonMobil Research and Engineering Co., Corporate Strategic Research Labs, Route 22 East, Annandale, NJ 08801, USA*

Received 29 November 2004; received in revised form 10 January 2005; accepted 23 February 2005

Abstract

The adsorption and desorption of thiophene and the reactions of thiophene-derived adsorbed species in He, H_2, and O_2 were examined on H-ZSM5, H-Beta, and H-Y with varying Si/Al ratios. Thiophene adsorption uptakes (per Al) were independent of Al content, but were above unity and influenced by zeolite structure (1.7, 2.2, and 2.9 on H-ZSM5, H-Beta, and H-Y). These data indicate that thiophene oligomers form during adsorption and that their size depends on spatial constraints within zeolite channels. Adsorption and oligomerization occur on Brønsted acid sites at 363 K. Thiophene/toluene adsorption from their mixtures show significant thiophene selectivity ratios (10.3, 7.9, and 6.4, for H-ZSM5, H-Beta, and H-Y zeolites), which exceed those expected from van der Waals interactions and reflect specific interactions with Brønsted acid sites and formation of toluene–thiophene reaction products. Treatment of thiophene-derived adsorbed species above 363 K in He or H_2 led to depolymerization of thiophene oligomers and to the formation of unsaturated adsorbed species with a 1:1 thiophene/Al stoichiometry on all zeolites and at all Si/Al ratios. These unsaturated species desorb as stable molecules, such as H_2S, hydrocarbons, and larger organosulfur compounds, formed via ring opening and hydrogen transfer from H_2 or co-adsorbed species, and also form stranded unsaturated organic deposits. Smaller channels and higher Al contents preferentially formed H_2S, benzotiophenes, and arene products during treatment in He or H_2, as a result of diffusion-enhanced of secondary reactions of desorbed thiophene molecules with adsorbed thiophene-derived species. Only oxidative regeneration treatments led to full recovery of thiophene uptake capacities. A preceding treatment in H_2, however, led to the partial recovery of thiophene-derived carbon atoms as useful hydrocarbons and decreased the amount of CO_2 and SO_2 formed during subsequent oxidative treatments required for regeneration.
© 2005 Published by Elsevier B.V.

Keywords: Thiophene; Zeolites; Adsorption; Desorption; Oligomerization; Regeneration

1. Introduction

Organosulfur compounds in fuels cause toxic emissions and inefficient performance of exhaust catalysts [1–3]; thus, processes for their removal have been widely explored [4–20]. Selective adsorption [21–31] can be carried out at low temperatures; they avoid saturation of alkenes and arenes, which prevail during hydrodesulfurization catalysis, but available materials show limited adsorption capacities and selectivities. Thiophene, benzothiophene, and their alkyl derivatives are the most abundant organosulfur compounds in gasoline; more reactive sulfides, disulfides, and mercaptans are present as minor components. Thiophene represents a particular challenge, because it resembles abundant arenes and alkenes in electron density and basicity, thus making chemical specificity difficult during adsorption and catalysis. The crystalline framework structure, high specific area, and structural and compositional flexibility make zeolites potential candidates for thiophene adsorption [32]. Thiophene adsorbs on H-ZSM5 [28] with modest selectivity relative to benzene; samples with high Al-content showed high adsorption capacities for thiophene and alkyl-thiophenes, indicating specific interactions with Al sites and possible acid-catalysed alkylation reactions with alkenes or other components to form larger organosulfur compounds [31]. Y-zeolites

* Corresponding author. Tel.: +1 510 642 9673; fax: +1 510 642 4778.
E-mail address: iglesia@cchem.berkeley.edu (E. Iglesia).

0926-3373/$ – see front matter © 2005 Published by Elsevier B.V.
doi:10.1016/j.apcatb.2005.02.031

exchanged with Cu or Ag cations selectively adsorb thiophene from benzene via specific π-interactions [25,33,34].

We recently reported a detailed study of thiophene adsorption and reactions on H-ZSM5, including reactions of thiophene-derived adsorbed species O_2, He, H_2, and C_3H_8 [35]. Acid sites were partially restored with H_2 or C_3H_8 treatments to recover most thiophene-derived carbons as useful hydrocarbons.

The structure and Al content of zeolites influence both adsorption capacity and regeneration pathways during thiophene adsorption processes [36–41]. Here, we examine the effects of zeolite channel size and crystal structure on the adsorption and subsequent reactions of thiophene using MFI, BEA, and FAU zeolites with similar Al content (Si/Al = 13); we also probe the effects of Al content in FAU structures (Si/Al = 6, 13, 33, and 85). Finally, we report thiophene adsorption stoichiometries on MFI, BEA, and FAU zeolites during adsorption, which are consistent with reversible oligomerization reactions during adsorption and thermal treatment, and the rates and selectivities in reactions of adsorbed thiophene-derived species during thermal treatments in He and H_2 streams.

2. Experimental methods

2.1. Zeolite-based adsorbents

Faujasite zeolites with three-dimensional 12-ring channels were used in their acid form. H-Y samples [H-Y(6) (Si/Al = 6, MC-5879), H-Y(13) (Si/Al = 13, MC-5876), H-Y(33) (Si/Al = 33, MC-5877), and H-Y(85) (Si/Al = 85, MC-58798)] were prepared by dealumination of high-silica ECR-32 with H_4EDTA and by sequential steaming and acid treatments using previously reported methods [42,43]. ECR was first prepared from a starting gel of composition, 9.6 TPAOH:1.6 Na_2O:Al_2O_3:24 SiO_2:350 H_2O:0.72 Na_2SO_4, where tetrapropylammonium hydroxide (TPAOH) and 10% of the alumina came from a seed solution with a SiO_2:Al_2O_3 ratio of 17.5. The recovered solids had a Si/Al atomic ratio of 5.1 and were calcined in dry air for 3 h at 873 K to remove organic template. One portion (100 g) was placed in refluxing H_2O (1500 g) for 20 h within a Soxhlet extractor, while slowly adding H_4EDTA (30.3 g) [43]. The product was recovered by filtration and washed with distilled H_2O. This dealuminated sample was converted to its proton form by four sequential 1 h exchanges with 10% NH_4Br solutions at 333 K. After the second and third exchanges, samples were treated in dry air at 623 K for 3 h. This sample gave a Si/Al ratio of 13 (by ICP-AES) and is denoted as H-Y(13). A second portion of the calcined ECR-32 was converted to its proton form by the procedure described above. After the second and third exchanges, samples were treated in dry air at 573 K for 3 h, a procedure that led to a Si/Al ratio of 6; this sample is denoted as H-Y(6). One portion of this second sample was then treated (175 g) with water vapor at 1 bar and 950 K for 5 h and then contacted with 0.5N HCl (2.63 L) under reflux for 3 h. The product was recovered by filtration and washed with distilled H_2O to give a sample with a Si/Al ratio of 85 [H-Y(85)].

A sample similar to H-Y(85) was prepared using a material prepared from a mother liquor recycle synthesis of ECR-32 as the starting material [44]. After treatment in dry air at 573 K for 3 h, this sample was exchanged with NH_4^+ and steamed by the same procedure as H-Y(85). The sample (10 g) was then treated in 150 cm^3 1.0N HCl under reflux for 4.5 h. The product was recovered by filtration and washed with distilled H_2O to give a Si/Al ratio of 33 [H-Y(33)]. A schematic description of the synthesis protocols is presented below.

Two H-Beta samples [H-Beta(13) (Si/Al = 13, CP814E) and H-Beta(38) (Si/Al = 38, CP811E)] were obtained from Zeolyst Corp. in NH_4^+ and H^+ forms, respectively. H-ZSM5(13) (Si/Al = 13, Lot 97EB-6197) was obtained from AlSi-Penta Corp. in NH_4^+ form. H-ZSM(40) (Si/Al = 40, CBV-5014) was obtained from Zeolyst Corp. in H^+ form. NH_4^+ zeolites were converted into their respective H^+ form by treatment in flowing dry air at 773 K for 3 h (Airgas, C.P. > 99.9%, 1.7 $cm^3\ s^{-1}$). Chemical compositions, crystallite sizes, and pore volumes for H-Beta and H-ZSM5 zeolites are shown in Table 1; these data were provided by Zeolyst Corp. and AlSi-Penta Corp., respectively. Pore volumes of H-Y zeolites were measured from *n*-hexane adsorption isotherms (Cahn 2000 vacuum microbalance)

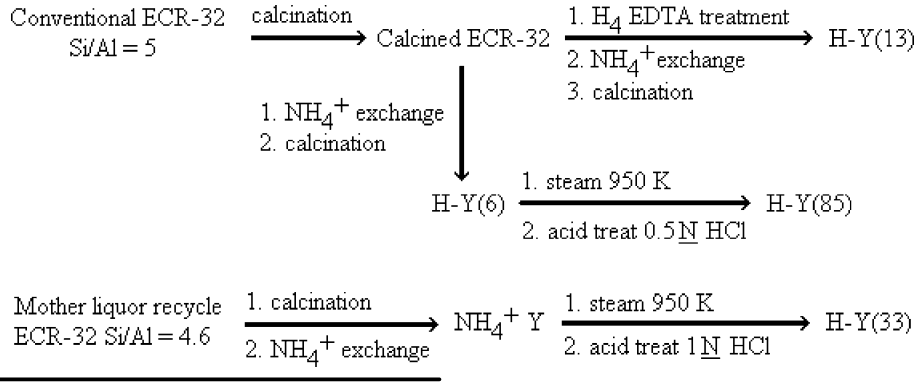

Table 1
Physicochemical properties of H-ZSM5, H-Beta, and H-Y zeolites

	H-ZSM5(13)	H-ZSM5(40)	H-Beta(13)	H-Beta(38)	H-Y(6)	H-Y(13)	H-Y(33)	H-Y(85)
Zeolite structure	Pentasil (MFI)	Pentasil (MFI)	Beta (BEA)	Beta (BEA)	Faujasite (FAU)	Faujasite (FAU)	Faujasite (FAU)	Faujasite (FAU)
Pore size (nm)	0.53 × 0.56 0.51 × 0.55	0.53 × 0.56 0.51 × 0.55	0.66 × 0.67 0.56 × 0.56	0.66 × 0.67 0.56 × 0.56	0.74 × 0.74	0.74 × 0.7 4	0.74 × 0.7 4	0.74 × 0.74
Particle size (nm)	200	250	200	200	200	300	500	400
Si/Al	13	40	13	38	6	13	33	85
Na/Al	0.008	0.009	<0.002	<0.002	<0.001	<0.001	<0.002	<0.002
Fe/Al	0.005	0.005	<0.0001	<0.0002	<0.0001	<0.0001	<0.0001	<0.0001
Surface area (m^2/g)[a]	400	425	680	650	–	–	–	–
Pore volume (cm^3/g)	0.128	0.129	0.189	0.1290	0.302	0.326	0.311	0.301
$Al_{framework}/Al_{total}$[b]	0.91	–	–	–	0.91	0.92	1.0	0.84

Calculated from ^{27}Al MNR analysis.
[a] Surface area data supplied by Zeolyst and AlSi-Penta Corp. and based on BET method.
[b] Framework Al/total Al ratio of calcined sample.

after treating samples in dynamic vacuum ($<10^{-5}$ kPa) at 673 K overnight. Crystallite sizes were measured by scanning electron microscopy (Phillips XL-40) and framework Al contents were estimated from solid-state ^{27}Al MAS NMR spectra at ambient temperature (Bruker AMX-360 spectrometer). Each sample was pelleted and sieved into granules with 135–180 μm diameter before thiophene adsorption reaction measurements.

2.2. Thiophene adsorption–desorption measurements

Thiophene adsorption uptakes were measured at 363 K in a quartz cell using a packed-bed of zeolite (0.25 g) treated in flowing dry air (Airgas, C.P. > 99.9%, 1.7 $cm^3\ s^{-1}$) at 773 K for 1 h and cooled to 363 K in He/Ar (Matheson, He/Ar (95/5), 1.7 $cm^3\ s^{-1}$). Thiophene (Aldrich, >99%) was introduced into a heated line using a syringe pump (Cole Palmer 74900). Samples were exposed to thiophene in He/Ar flow at 363 K. After removing thiophene from the flow stream, weakly adsorbed thiophene molecules were removed by He/Ar (Matheson, He/Ar (95/5), 1.7 $cm^3\ s^{-1}$) flow at 363 K for 0.25 h. Thiophene concentrations were measured continuously by mass spectrometric analysis of the effluent stream (Leybold Inficon Inc. Transpector). All the thiophene in the inlet stream was adsorbed during the early stages of contact, until thermodynamic equilibrium was reached, at which time thiophene concentration gradually increased with time and ultimately reached inlet values. Adsorption uptakes were determined from the difference between inlet and outlet thiophene concentrations integrated over time.

The rate of removal of adsorbed species by desorption or reaction was measured using He (Airgas, >99.99%, 1.7 $cm^3\ s^{-1}$) or H_2 (Airgas, >99.99%, 1.7 $cm^3\ s^{-1}$) as carriers while temperature was raised from 363 to 773 K at 0.42 $K\ s^{-1}$. Effluent concentrations of thiophene and reaction products were measured continuously by mass spectrometry and intermittently by gas chromatography (Hewlett-Packard 6890, capillary HP-1 cross-linked methylsilicone column, 50 mm × 0.32 mm, 1.05 μm film, packed

Table 2
Comparison of total amount of adsorbed thiophene, thiophene removed during flushing, thiophene retained after flushing at 363 K, thiophene desorbed as unreacted thiophene, thiophene desorbed as other products and thiophene retained after regeneration of H-ZSM5(13), H-Beta(13), and H-Y(13) zeolites using He or H_2 as carrier gases

Total thiophene adsorbed (per Al)	Thiophene removed during flushing at 363 K (per Al)	Thiophene retained after flushing at 363 K (per Al)	Regeneration carrier gas (1.7 $cm^3\ s^{-1}$)	Thiophene desorbed unreacted (per Al)	Thiophene desorbed as other products (per Al)	Thiophene retained after regeneration (per Al)
H-ZSM5(13)						
2.05	0.3	1.75	**He**	0.59	0.11	1.05
2.01	0.35	1.66	**H_2**	0.75	0.14	0.91
H-Beta(13)						
2.68	0.49	2.19	**He**	0.99	0.09	1.11
2.64	0.53	2.11	**H_2**	1.03	0.15	0.93
H-Y(13)						
3.48	0.64	2.84	**He**	1.56	0.10	1.18
3.49	0.59	2.90	**H_2**	1.67	0.16	1.07

Adsorption conditions: 363 K, 1 kPa thiophene, balance He. Desorption conditions: heating rate of 0.42 $K\ s^{-1}$ and final regeneration temperatures of 773 K.

Hayesep-Q column, 80/100 mesh, 10 in. × 0.125 in.) using flame ionization and thermal conductivity detection.

3. Results and discussion

3.1. Thiophene adsorption measurements

Thiophene adsorption uptakes on three zeolite structures with similar Al contents [H-ZSM5(13), H-Beta(13), and H-Y(13)] are shown in Table 2. After reaching equilibrium uptakes, samples were treated with He at 363 K (1.7 $cm^3\ s^{-1}$) for 0.25 h to remove weakly adsorbed species; only thiophene was detected in the effluent during this treatment [0.3, 0.5, and 0.6 desorbed thiophene/Al on H-ZSM5(13), H-Beta(13), and H-Y(13), respectively]. Uptakes of strongly adsorbed thiophene were measured from the difference between the amounts of thiophene adsorbed and desorbed during treatment in He at 363 K.

Strongly adsorbed thiophene uptakes were 1.7, 2.2, and 2.9 thiophene/Al on H-ZSM5(13), H-Beta(13), and H-Y(13), respectively, at 363 K and 1 kPa thiophene (Table 2), indicating that adsorption stoichiometries depend on channel size and zeolite structure. These uptakes were much lower than those required to fill zeolite channels with condensed thiophene, which were estimated to be 2.8, 4.1, and 7.0 for H-ZSM5, H-Beta, and H-Y, for a thiophene molecular volume of 0.65 nm^3 (estimated using Chem3D Pro; CambridgeSoft, using energy minima and a MM2 field). Thiophene uptakes were also measured on samples with different Al contents [H-ZSM5 (Si/Al = 13, 40), H-Beta (Si/Al = 13, 38), and H-Y (Si/Al = 6, 13, 33, and 85)]. Table 3 shows that adsorption stoichiometries were essentially independent of Al content for a given zeolite and above unity on all samples. This appears to reflect the formation of thiophene oligomers, the size of which depends on spatial constraints within zeolite channels.

The role of van der Waals interactions was probed by measuring adsorption uptakes on H-ZSM5(13), H-Beta(13), and H-Y(13) as a function of thiophene pressure (0.25–2 kPa) and 363 K. Uptakes were accurately described by

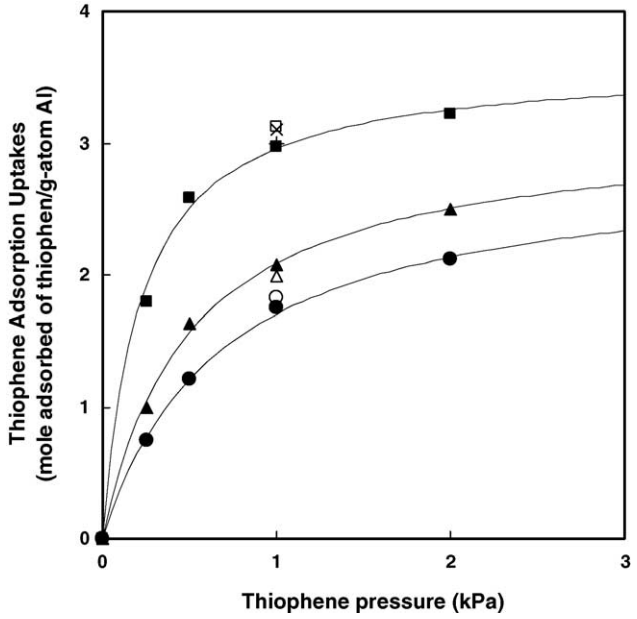

Fig. 1. Adsorption isotherms for thiophene on H-ZSM5(13), H-Beta(13), and H-Y(13) zeolites at 363 K. The points represent experimental data: (●) H-ZSM5(13) (Si/Al = 13), (○) H-ZSM5(40) (Si/Al = 40), (▲) H-Beta(13) (Si/Al = 13), (△) H-Beta(38) (Si/Al = 38), (■) H-Y(13) (Si/Al = 13), (×) H-Y(6) (Si/Al = 6), (+) H-Y(33) (Si/Al = 33), (□) H-Y(85) (Si/Al = 85). The curves represent the calculated fitted Langmuir-type isotherms (Eq. (1)).

Langmuir isotherms (Eq. (1), Fig. 1, Table 4), consistent with minimal contributions from physisorbed thiophene [45–47]:

$$C_{ads} = \frac{C_t K_1 P_{th}}{1 + K_1 P_{th}} \quad (1)$$

where K_1 is an equilibrium adsorption constant, C_t the total number of bound thiophene at saturation, and P_{th} is the thiophene pressure. K_1 and C_t values were largest on H-Y and smallest on H-ZSM5 (Table 4), suggesting that thiophene binding energies and stoichiometries depend on zeolite structure. For each zeolite structure, adsorption stoichiometries were not influenced by Al content (Table 4), but were greater than unity for all samples. Taken together with the apparent

Table 3
Thiophene retained after flushing with He [363 K and 1.7 $cm^3\ s^{-1}$ He for 0.25 h] and retained after regeneration in He as carrier gas [500 K, 1.7 $cm^3\ s^{-1}$ He for 1 h] on H-ZSM5, H-Beta, and H-Y zeolites with different Si/Al ratios

Zeolite	Si/Al	Thiophene retained after flushing with He (1.7 $cm^3\ s^{-1}$) at 363 K (per Al)	Thiophene retained after regeneration in He (1.7 $cm^3\ s^{-1}$ He) at 773 K (per Al)
H-ZSM5(13)	13	1.75	1.05
H-ZSM5(40)	40	1.81	1.07
H-Beta(13)	13	2.20	1.11
H-Beta(38)	38	2.17	1.12
H-Y(6)	6	3.05	1.18
H-Y(13)	13	2.94	1.18
H-Y(33)	33	2.98	1.18
H-Y(85)	85	3.02	1.21

Table 4
Thiophene adsorption parameters for H-ZSM5(13), H-Beta(13), and H-Y(33) zeolites at 363 K

Sample	Si/Al (mol)	Saturation thiophene uptakes (C_t) (thiophene/Al)	K_A[a] (kPa^{-1})
H-ZSM5(13)	13	2.86	1.5
H-Beta(13)	13	3.13	2.0
H-Y(13)	13	3.59	4.6

[a] Adsorption coefficient in Langmuir isotherm.

absence of physisorbed thiophene, which would have desorbed during He treatment at these temperatures, these data suggest that thiophene oligomers form on Brønsted acid sites during adsorption at 363 K.

Infrared spectra of thiophene adsorbed on H-ZSM5 (Si/Al = 14.5) by Yu et al. [49] and on H-Y (Si/Al = 5.4) by Geobaldo et al. [48] at ambient temperature detected the formation of thiophene oligomers during adsorption. Thiophene reacts via electrophilic addition in phosphoric acid to form predominantly trimers [50,51] while it forms larger oligomers on cation-exchanged Y-zeolite and mordenite [52] and on montmorillonite [53]. Thus, the formation of thiophene oligomers through chemical reaction of protonated thiophene appears to account for the measured adsorption stoichiometry values above unity.

Thiophene adsorption stoichiometries increased with increasing zeolite pore volume (MFI = 0.13 cm^3/g, BEA = 0.19 cm^3/g, FAU = 0.31 cm^3/g) and channel size (MFI: 0.51 nm × 0.55 nm and 0.53 nm × 0.56 nm, BEA: 0.66 nm × 0.67 nm and 0.56 nm × 0.58 nm, FAU: 0.74 nm × 0.74 nm), suggesting that the extent of oligomerization is influenced by spatial constraints within channels.

3.2. Competitive adsorption reactions of thiophene–toluene mixtures

Adsorption selectivities were measured from competitive adsorption of thiophene–toluene mixtures [363 K, 0.15 kPa thiophene, 3.0 kPa toluene]. Uptakes of strongly adsorbed thiophene were 0.19, 0.26, and 0.26 thiophene/Al on H-ZSM5(13), H-Beta(13), and H-Y(13), respectively; these uptakes are much lower that those measured at this thiophene pressure without toluene (0.52, 0.72, and 1.46 thiophene/Al, respectively). Thiophene adsorption selectivity (relative to toluene), defined as:

$$S_{Th} = \frac{X_{Th}/P_{Th}}{X_{Tol}/P_{Tol}} \quad (2)$$

where X_{Th} and X_{Tol} are the moles of thiophene and toluene adsorbed per Al and P_{Th} and P_{Tol}, partial pressures of thiophene and toluene, were 10.3, 7.9, and 6.4 on H-ZSM5(13), H-Beta(13), and H-Y(13). These selectivities are greater than unity, consistent with the greater gas phase basicity of thiophene relative to toluene (784 kJ/mol versus 756 kJ/mol [54]), but indicate some influence of zeolite channel size on selectivity. Thus, H-ZSM5 adsorbs thiophene more selectively than H-Beta and H-Y even though the smaller channels on H-ZSM5 restrict the size of adsorbed thiophene oligomers. These selectivity values exceed those expected from physisorption processes, which would solely reflect the ratio of the saturation vapor pressures for thiophene and toluene (2.2 at 363 K [55,56]); thus, binding appears to involve specific chemical interactions and, in view of the observed stoichiometries, even chemical reactions.

After these competitive adsorption measurements, samples were treated in H_2 while increasing the temperature from 363 to 773 K at 0.42 K s^{-1}. Toluene desorbed at low temperatures (500 K) with toluene/Al ratios of 0.30, 0.51, and 0.63 on H-ZSM5(13), H-Beta(13), and H-Y(13). These values are slightly lower than toluene uptakes measured

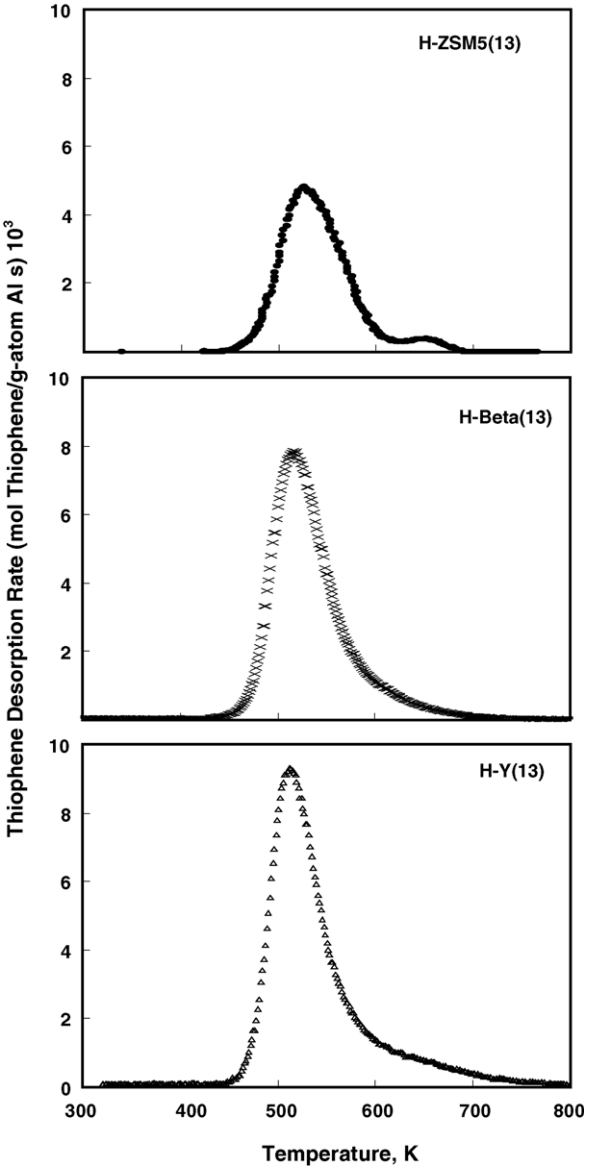

Fig. 2. Thiophene desorption rates during regeneration of H-ZSM5(13), H-Beta(13), and H-Y(13) using H_2 as carrier gas [Si/Al = 13, 0.42 K s^{-1}, isothermal at 773 K, 1 h].

Table 5
Total amount of desorbed products (10^3 × mol products/g atom of Al) during regeneration of H-ZSM5(13), H-Beta(13), H-Y(13), H-Y(6), H-Y(33), and H-Y(85) with He or H_2 [heating rate of 0.417 K s^{-1}, isothermal at 773 K, 1 h]

Compounds	H-ZSM5(13)		H-Beta(13)		H-Y(13)		H-Y(6)		H-Y(33)		H-Y(85)	
	He	H_2	He	H_2	He	H_2	He	H_2	He	H_2	He	H_2
Ethene	5.9	8.7	4.8	7.3	4.9	7.9	5.6	8.3	3.6	6.6	2.2	4.7
Propene	3.7	6.1	31.1	51.6	37.8	59.9	39.8	61.6	37.6	58.6	35.6	57.4
Benzene	5.8	9.3	3.4	5.2	1.8	3.1	2.4	4.1	1.4	2.6	0.9	1.6
Toluene	4.9	6.4	2.3	3.3	2.3	5.1	3.1	6.2	2.1	3.9	1.6	2.4
Thiophene	590.0	750.0	989.3	1126.3	1555.3	1656.9	1548.3	1643.3	1562.3	1671.2	1571.3	1698.3
Methylthiophene	3.2	5.7	30.8	52.5	37.1	58.5	40.5	62.3	37.6	57.8	36.6	56.6
Benzothiophene	42.1	48.1	10.5	14.2	8.4	10.7	9.1	11.3	8.1	0.3	8.1	9.6
H_2S	307.1	460.0	446.3	602.6	535.6	753.2	571.3	792.1	510.2	709.1	493.2	658.3
AC/OSC[a]	0.24	0.29	0.14	0.13	0.09	0.12	0.11	0.14	0.08	0.10	0.06	0.06

[a] AC, aromatic compounds (benzene + toluene); OSC, organosulfur compounds (methylthiophene + benzothiophene)

during initial contact of these samples with toluene–thiophene mixtures [0.37, 0.66, and 0.81 for H-ZSM5(13), H-Beta(13), and H-Y(13)] indicating that some adsorbed toluene reacted with thiophene or with other toluene molecules to form strongly held species. No specific products of thiophene–toluene reactions were detected in the effluent, but this may just reflect their inability to desorb at these treatment temperatures. At higher temperatures (>530 K), traces of

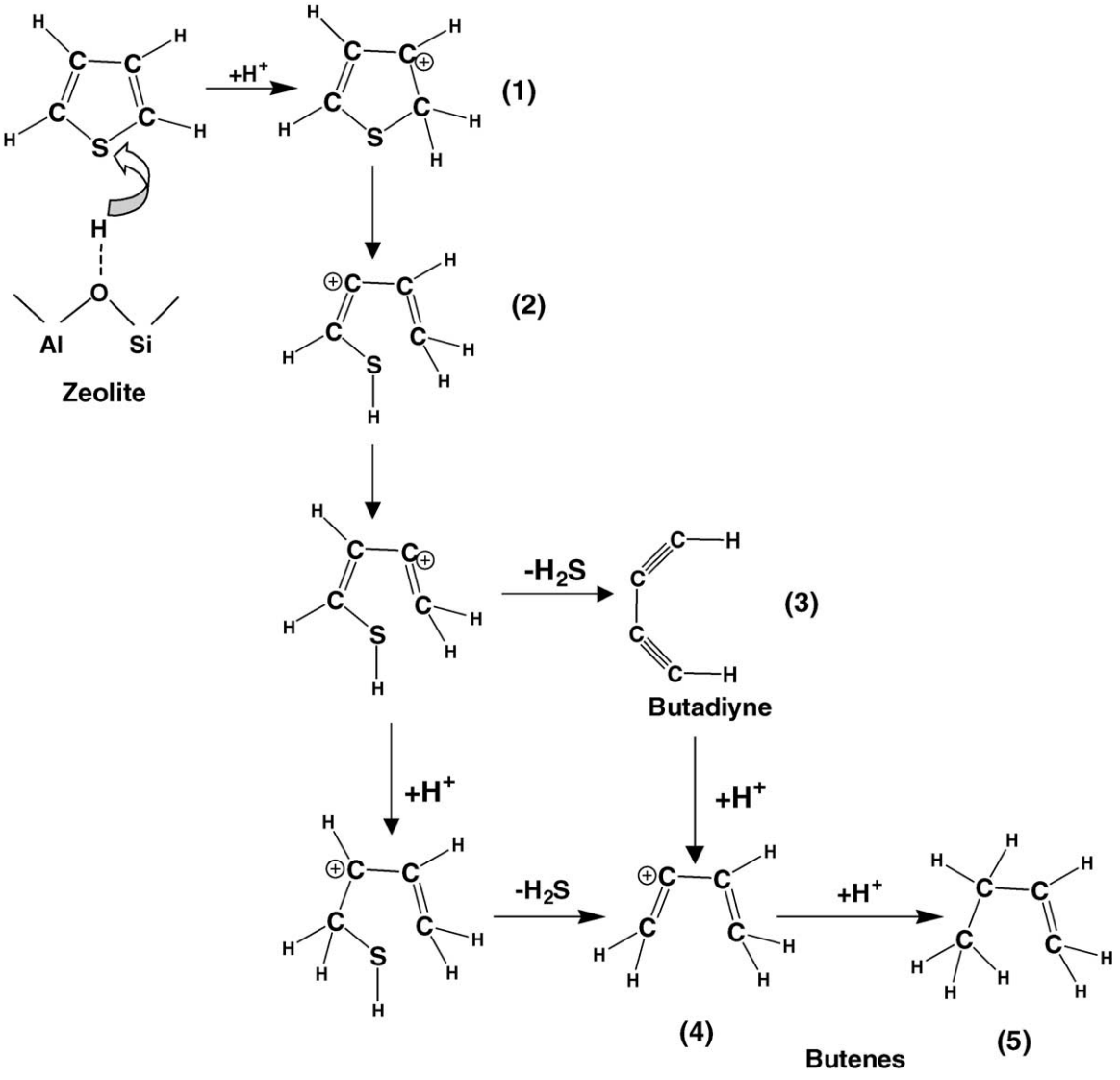

Scheme 1. Thiophene ring activation, ring opening reaction, and formation of H_2S and C_4 fragments.

unreacted thiophene and of thiophene reaction products (benzene, toluene, methylthiophene, and benzothiophene) were detected. Uptakes during competitive adsorption of thiophene and toluene were also measured on H-Y zeolites with varying Si/Al ratios (Si/Al = 6, 13, 33, and 85). Thiophene adsorption selectivities were unaffected by Al content (6.6, 6.4, 6.5, and 6.6 on H-Y(6), H-Y(13), H-Y(33), and H-Y(85)). Thus, competitive adsorption of toluene and thiophene reflect specific interactions with Brønsted acid sites and the formation of adsorbed species via toluene–thiophene reactions on acid sites; these species appear to remain adsorbed during subsequent thermal treatments.

3.3. Thiophene desorption from H-ZSM5, H-Beta, and H-Y in He or H_2 carriers

The dynamics of desorption and chemical reactions of adsorbed thiophene-derived species were measured on H-ZSM5(13), H-Beta(13), H-Y(6), H-Y(13), H-Y(33), and H-Y(85) in He or H_2 carrier gases. Weakly adsorbed thiophene was removed in He flow at 363 K for 0.25 h and the temperature then increased at 0.42 K s^{-1} to 773 K and held for 1 h. Unreacted thiophene evolved from H-ZSM5(13) as two desorption peaks (at 534 and 668 K) with He and H_2 carriers while only one peak was detected in H-Beta(13) and H-Y (at 525 K, Fig. 2). The low-temperature peak in H-ZSM5 has been attributed to the desorption of physisorbed thiophene, while the higher temperature peak reflects specific interactions of thiophene with protons or metal cations (e.g. Na^+, Fe^{3+}) [35,49,57]. Thiophene/Al desorbed in the second peak (~0.01) resembles the (Na + Fe)/Al ratio (0.013) in H-ZSM5(13), consistent with a role of these cations in the reversible binding and molecular desorption of thiophene. In H-Beta(13) and H-Y (Si/Al = 6, 13, 33, and 85), (Na + Fe)/Al ratios are much lower (<0.003; Table 1) and the second desorption peak is not detected. Thiophene desorbs from H-Beta(13) and H-Y (Si/Al = 6, 13, 33, and 85) at temperatures similar to those observed on H-ZSM5(13). Thus, pore size, geometry, and chemical composition do not significantly influence the desorption temperature of unreacted thiophene, which reflects that required for the depolymerization of thiophene oligomers, as discussed below.

The amounts of thiophene desorbed unreacted (per Al) in He or H_2 were highest on H-Y and lowest on H-ZSM5 (Table 5), consistent with the higher thiophene uptakes observed during adsorption on H-Y. The amounts of thiophene-derived adsorbed species remaining after treatment at 773 K in He or H_2 correspond to thiophene/Al ratios near unity for all samples (0.9–1.2 thiophene/Al, Tables 2 and 3), irrespective of channel structure or Al content. These results suggest a specific stoichiometric interaction of thiophene with acidic OH groups in zeolites to form strongly-bound unsaturated residues, which desorb as stable products only after hydrogenation, using sacrificial co-adsorbed species or H_2, or via combustion reactions in O_2-containing streams.

H_2S, ethene, propene, benzene, toluene, methylthiophene, and benzothiophene were detected as products on all samples during treatment of adsorbed thiophene in either He or H_2 (Table 5). H_2S forms at low temperatures (~520 K) via C–S bond cleavage in thiophene-derived carbocations to form unsaturated fragments on Brønsted acid sites [47,52–58] (Scheme 1, 1). These low-temperature H_2S formation pathways are consistent with ring-opening reactions that form adsorbed intermediates detected by infrared spectroscopy near ambient temperatures [45] and leading to H_2S and adsorbed butadiyne (C_4H_2) species (Scheme 1, 3). The amount of H_2S desorbed (per Al) for H-Y increased with Al

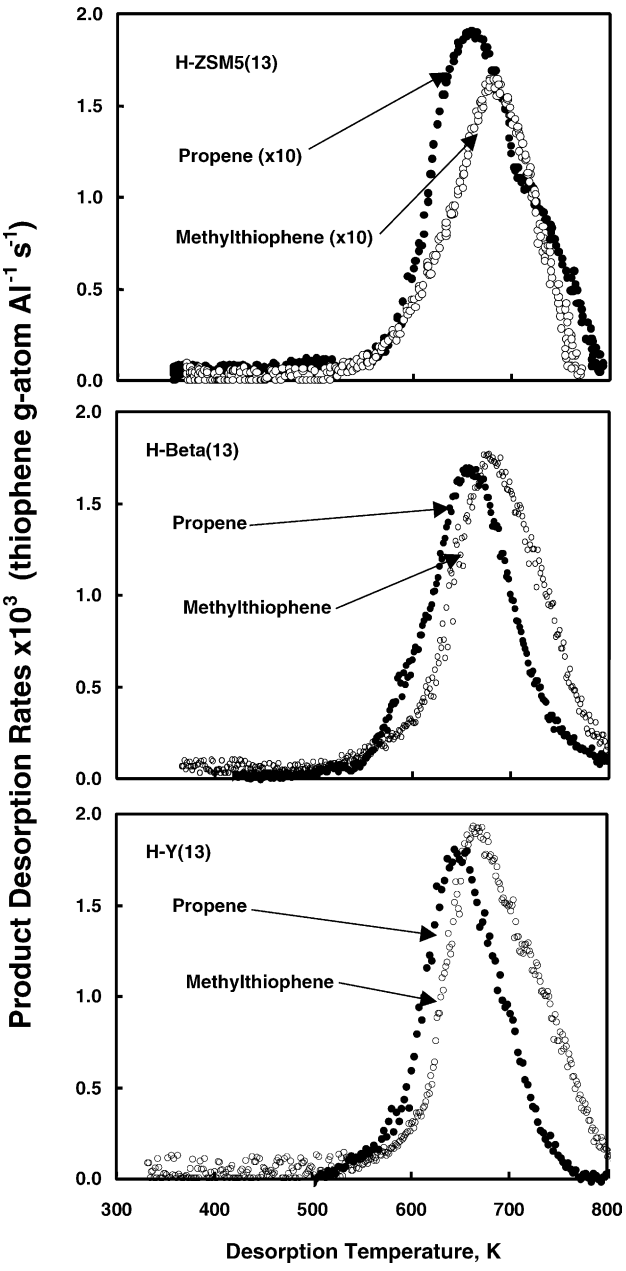

Fig. 3. Methylthiophene and propene desorption rates during regeneration of H-ZSM5(13), H-Beta(13), and H-Y(13) using H_2 as carrier [Si/Al = 13, 0.42 K s^{-1}, isothermal at 773 K, 1 h].

content, apparently because desorbed thiophene molecules have a higher probability of reacting with other adsorbed thiophene to form H_2S via bimolecular Diels–Alder-type reactions as the number of adsorption sites increases with increasing Al content. These effects of Al content were also observed on H-ZSM5 [0.325 H_2S/Al on H-ZSM5(40); 0.460 H_2S/Al for H-ZSM5(13)].

Benzene, toluene, benzothiophene, and ethene formed in smaller amounts on H-Beta and H-Y than on H-ZSM5. Larger amounts of methylthiophene and propene (Table 5) formed on H-Beta and H-Y than on H-ZSM5. The similar desorption profiles and molar amounts of methylthiophene and propene suggest that they form via common intermediates and pathways (Fig. 3 and Table 5). Ring-opened intermediates formed from thiophene concurrently with H_2S evolution can react with thiophene molecules as they desorb to form adsorbed butyl-thiophene species, after isomerization and hydrogen transfer (Scheme 2, 8 or 9); these species

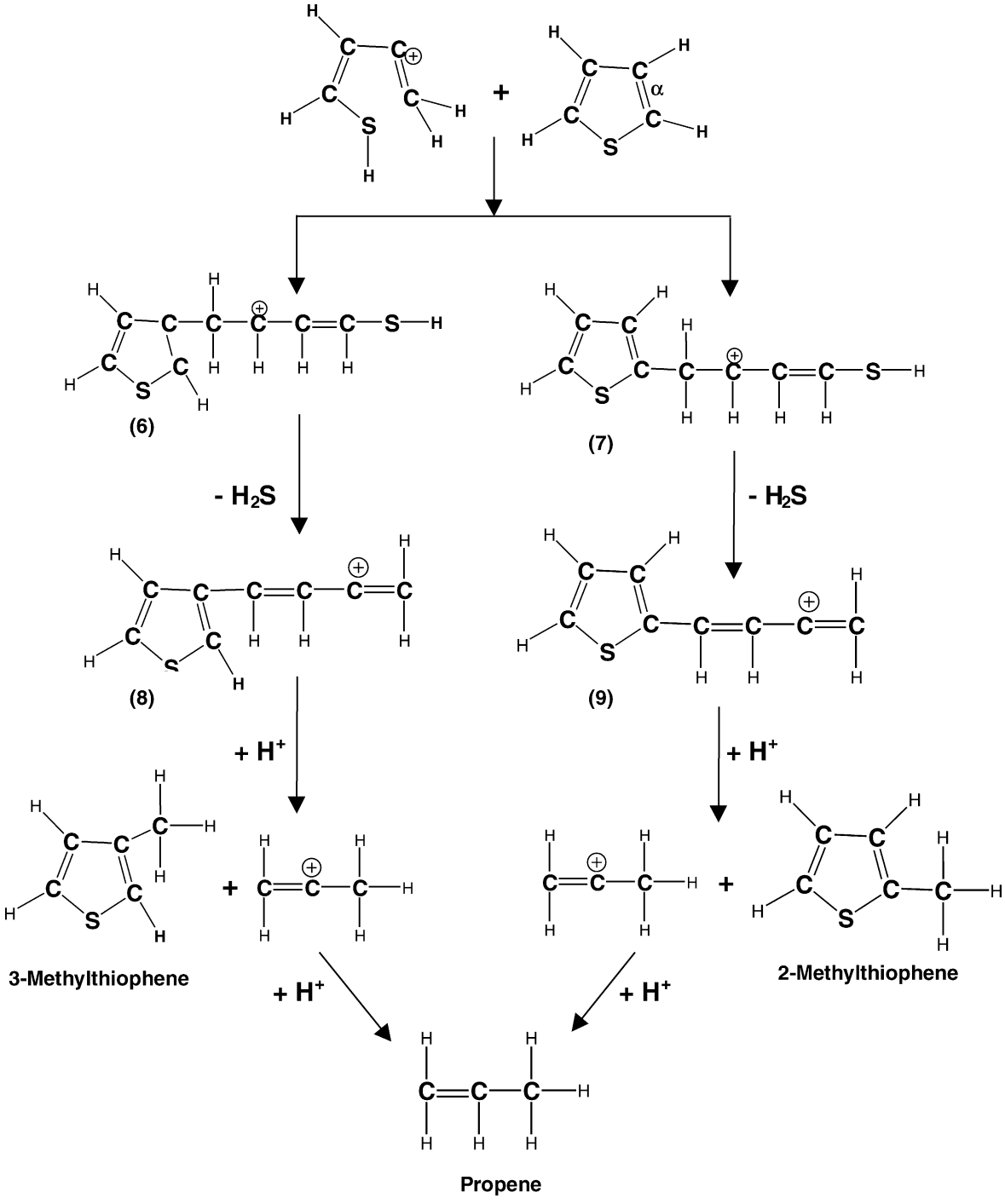

Scheme 2. Methylthiophene and propene formation pathway.

Table 6
Comparison of the amount of thiophene adsorbed, removed by H_2, retained at 363 K, desorbed amounts of CO_2 and SO_2 during the subsequent treatment in O_2 [O_2/He (20/80, mol), 1.7 $cm^3\ s^{-1}$], thiophene adsorbed at 363 K in the zeolite after treatment with O_2 and recovered adsorption capacity after oxidative treatment

Sample	Thiophene retained after flushing with He at 363 K (molecules/Al)	Thiophene retained after regeneration in H_2 at 773 K (molecules/Al)	Amount of desorbed products during the subsequent oxidative treatment at 873 K (molecules/Al)		Thiophene retained (after flushing with He at 363 K) on the regenerated sample after the oxidative treatment	Recovered adsorption capacity[c] (%)
			CO_2[a]	SO_2[b]		
H-ZSM5(13)	1.75	0.91	3.76	0.48	1.73	98.8
H-Beta(13)	2.19	0.83	3.72	0.42	2.23	∼100
H-Y(13)	2.90	1.07	3.96	0.40	2.89	99.7

[a] CO_2 amounts have been directly measured by mass spectrometry.
[b] SO_2 amounts have been estimated from a sulfur balance. It was assumed that all the remaining S in the zeolite after H_2 treatment reacts with O_2 to form SO_2.
[c] Recovered adsorption capacity was calculated as: [(thiophene adsorbed after oxidation treatment (after flushing at 363 K))/(thiophene adsorbed on the fresh catalyst after flushing at 363 K)] × 100.

can form methyl-thiophene and propene with a 1:1 stoichiometry after hydrogen transfer [59–61]. Methylthiophene forms via alkylation reactions (Scheme 2, 9), involving bulky transition states that appear to be favoured within larger channels in H-Y and H-Beta. In contrast, the slower formation and diffusion of methylthiophene within smaller H-ZSM5 channels would enhance its interactions with acid sites or adsorbed thiophene-derived species to form desorbable molecules, such as benzene, toluene, benzothiophene, and propane.

Regeneration in He or H_2 did not completely remove all adsorbed thiophene-derived species (Table 2) or recover initial adsorption capacities. Initial capacities were recovered only after treatment with O_2-containing streams [O_2/He (20/80, mol), 1.7 $cm^3\ s^{-1}$]. After treatment with He or H_2, samples were cooled to 363 K and treated in O_2 by heating samples at 873 K for 1 h. Product evolution rates were measured by mass spectrometry during treatment in O_2 and CO_2 and SO_2 were the only products detected. Recovery of initial capacities was determined by a second thiophene adsorption measurement after each treatment. Table 6 shows that all samples recovered initial adsorption capacities after treatment in O_2 at 873 K. Treatment in H_2 did not fully restore initial capacities, but led to the recovery of thiophene-derived carbon atoms as useful hydrocarbons. As a result, subsequent oxidative treatments, which restore initial capacities, form less CO_2 and SO_2 than treatments of these samples without a prior treatment in H_2 (40% less of CO_2 and 80% less of SO_2).

4. Conclusions

The influence of structure and Si/Al ratio of H-ZSM5, H-Beta, and H-Y zeolites on the adsorption and subsequent desorption/reaction of thiophene was examined. Thiophene adsorption stoichiometries were higher than unity (1.7, 2.2, and 2.9 thiophene/Al for H-ZSM5, H-Beta, and H-Y zeolites), but independent of Si/Al ratio for each zeolite structure. Thiophene adsorption obeyed Langmuir isotherms, indicating that thiophene adsorbs via strong and specific interactions with Brønsted acid sites. Thiophene oligomers form during adsorption and account for thiophene/Al stoichiometries above unity, their size increases with increasing channel volume. Competitive adsorption of thiophene in toluene gave thiophene selectivities ratios (10.3, 7.9, and 6.4, for H-ZSM5, H-Beta, and H-Y zeolites). Thermal treatment in He or H_2 led to depolymerization of adsorbed thiophene oligomers with concurrent evolution of thiophene molecules. These depolymerization processes led to the residual formation of unsaturated species corresponding to a nearly 1:1 thiophene:Al stoichiometry. At higher temperatures, these unsaturated species led to the formation of arenes and alkenes using H-atoms from co-adsorbed species or H_2. H_2S and arene amounts formed during He or H_2 treatments increased with Al content and decreasing channel size, as a result of diffusional constraints that led to secondary reactions during thiophene desorption. Complete removal of adsorbed species was achieved only by oxidative treatments at 873 K after He or H_2 treatments. H_2 regeneration treatments allowed the recovery of a significant fraction of the carbon atoms in thiophene as useful hydrocarbons, while minimizing the amounts of CO_2 and SO_2 produced during subsequent oxidative treatments.

Acknowledgements

Antonio Chica gratefully acknowledges the Ministerio de Educación, Cultura y Deportes de España and the Council for International Exchange of Scholars (CIES) for a Fulbright Postdoctoral Fellowship. Karl G. Strohmaier acknowledges the technical assistance of Richard McEvoy and Mobae Afeworki in obtaining the SEM and NMR data reported here for Y-zeolites.

References

[1] EPA Staff Paper on Gasoline Sulfur Issues, US Environmental Protection Agency Office on Mobile Sources, 1998.
[2] R.F. Wormsbecher, G.D. Weatherbee, G. Kim, T.J. Dougan, National Petroleum Refiners Association Annual Meeting, San Antonio, 1993.
[3] G. Tobin, P. Gladman, Hydr. Eng. 1 (1996) 26.
[4] C. Song, X. Ma, Appl. Catal. B: Environ. 41 (2003) 207.
[5] S. Ma, L. Sun, C. Song, Catal. Today 77 (2002) 107.
[6] R.A. Plundo, T.C. Readal, J.M. Stom, US Patent 3,876,532 (1975), to Gulf Research Development Co.
[7] S.W. Shorey, D.A. Lomas, W.H. Keesdom, Hydrocarbon Process. 78 (11) (1999) 43.
[8] T.A. Ngyen, M. Skripek, AIChE Spring National Meeting, April 17–21, 1994.
[9] L.L. Upson, M.W. Schnaith, Oil J. 95 (49) (1997) 47.
[10] H.A. Zinnen, L.T. Nemeth, J.R. Holmgren, B.J. Arena, US Patent 5,5843,300 (1998), to UOP LLC.
[11] B.D. Alexander, G.A. Huff, V.R. Pradhan, W.J. Reagan, R.H. Cayton, US Patent 6,024,865 (2000), to BP-Amoco Corporation.
[12] N.A. Collins, J.C. Trewella, US Patent 5,599,441 (1997), to Mobil Oil Corporation.
[13] A. Treiber, P.M. Dansette, H. El Amri, J.P. Girault, D. Ginderow, J.P. Mornon, D. Mansuy, J. Am. Chem. Soc. 119 (1997) 1565.
[14] S. Otsuki, T. Nonaka, N. Takashima, W. Quian, A. Ishihara, T. Imai, T. Kabe, Energy Fuels 14 (2000) 1232.
[15] J. Palomeque, J.M. Clacens, F. Figueras, J. Catal. 211 (2002) 10–108.
[16] I. Funakoshi, T. Aida, US Patent 5,753,102 (1998), to Funakoshi I.
[17] S.E. Bonde, D. Chapados, W.L. Gore, G. Dolbear, E. Skov, NPRA 2000, Annual Meeting AM-00-25, San Antonio, TX, March 26–28, 2000.
[18] D.J. Monticello, W.R. Finnerty, Annu. Rev. Microbiol. 39 (1985) 371.
[19] A. Bhadra, J.M. Scharer, M. Moo-Yong, Biotechnol. Adv. 5 (1987) 1.
[20] M.K. Lee, J.D. Senius, M.J. Grossman, Appl. Environ. Microbiol. 61 (1995) 4362.
[21] R.L. Irvine, US Patent 5,730,860 (1998), to The Pritchard Co.
[22] S. Velu, M. Xiaoliang, C. Song, Ind. Eng. Chem. Res. 42 (2003) 5293.
[23] R.T. Yang, A.J. Hernandez-Maldonado, F.H. Yang, Science 301 (2003) 79.
[24] J.L. Sotelo, M.A. Uguina, V.I. Agueda, Stud. Surf. Sci. Catal. 142 (2002) 1579.
[25] A.J. Hernandez-Maldonado, R.T. Yang, Ind. Eng. Chem. Res. 42 (2003) 123.
[26] S. Velu, S. Watanabe, X. Ma, L. Sun, C. Song, Pet. Chem. Div. Prepr. 48 (2) (2003) 56.
[27] W. Wardencki, R. Staszewski, J. Chromatogr. 91 (1974) 715.
[28] J. Weitkamp, M. Schwark, S. Ernest, J. Chem. Soc. Chem. Commun. 16 (1991) 1133.
[29] A.B.S.H. Salem, Ind. Eng. Chem. Res. 33 (1994) 336.
[30] S. Velu, X. Ma, L. Sun, C. Song, Pet. Chem. Div. Prepr. 48 (2) (2003) 58.
[31] D.L. King, C. Faz, T. Flynn, SAE 2000 World Congress. Paper 200-01-0002, Society of Automotive Engineers. Detroit, MI, March 6–9, 2000, pp. 1–5.
[32] E. Davis Mark, Ind. Eng. Chem. Res. 30 (1991) 1675.
[33] A.J. Hernandez-Maldonado, R.T. Yang, J. Am. Chem. Soc. 126 (2004) 992–993.
[34] A. Takahashi, F.H. Yang, R.T. Yang, Ind. Eng. Chem. Res. 41 (2002) 2487–2496.
[35] A. Chica, K.G. Strohmaier, E. Iglesia, Langmuir 20 (2004) 10982.
[36] D. Nicholson, Anal. Chem. 34 (1962) 370.
[37] F. Wuld, M. Kobayashi, A.J. Heeger, Polym. Prepr. 25 (2) (1984) 257.
[38] V. Lorprayoon, R.A. Condrate, Appl. Spectrosc. 36 (6) (1982) 696.
[39] W. Li, S.Y. Yu, E. Iglesia, J. Catal. 203 (2001) 175–183.
[40] W. Li, S.Y. Yu, E. Iglesia, Stud. Surf. Sci. Catal. 130 (2000) 899–904.
[41] S.Y. Yu, W. Li, E. Iglesia, J. Catal. 187 (1999) 257.
[42] D.E.W. Vaughan, K.G. Strohmaier, US Patent 5,549,881 (1996).
[43] G.T. Kerr, J. Phys. Chem. 72 (1968) 2594.
[44] D.E.W. Vaughan, K.G. Strohmaier, US Patent 5,637,287 (1997).
[45] R.S. Drago, C.E. Webster, J.W. McGiluray, J. Am. Chem. Soc. 120 (1998) 538.
[46] C.E. Webster, A. Cottone III, R.S. Drago, J. Am. Chem. Soc. 121 (1999) 12127.
[47] C.E. Webster, A. Cottone III, R.S. Drago, Microporous Mesoporous Mater. 33 (1999) 291.
[48] F. Geobaldo, G.T. Palomino, S. Bordiga, Z. Zecchina, C.O. Arean, Phys. Chem. Chem. Phys. 1 (1999) 561–569.
[49] S.Y. Yu, J. Garcia-Martinez, W. Li, G.D. Meitzner, E. Iglesia, Phys. Chem. Chem. Phys. 4 (2002) 1241–1251.
[50] S.L. Meisel, G.C. Johnson, H.D. Hartough, J. Am. Chem. Soc. 72 (1950) 910.
[51] A.H. Jackson, Chemistry of heterocyclic compounds, in: E.C. Taylor, A. Weissenberg (Eds.), Interscience, vol. 48, Part I, John Wiley & Sons, New York, 1987, p. 305.
[52] P. Enzel, T. Bein, J. Chem. Soc. Chem. Commun. 12 (1989) 1326.
[53] V. Lorprayoon, R.A.S. Condrate, Appl. Spectrosc. 36 (1982) 696.
[54] E.P. Hunter, S.G. Lias, J. Phys. Chem. Ref. Data 27 (3) (1998) 413–656.
[55] C.B. Williamham, W.J. Taylor, J.M. Pignocco, F.D. Rossini, J. Res. Natl. Bur. Stand. 35 (1945) 219–244.
[56] G. Waddington, J.W. Knowlton, D.W. Scott, G.D. Oliver, S.S. Todd, W.N. Hubbard, J.C. Smith, H.M. Huffman, J. Am. Chem. Soc. 71 (1949) 797–808.
[57] C.L. Garcia, J.A. Lercher, J. Phys. Chem. 96 (1992) 2669.
[58] X. Saintigny, R.A. van Santen, S. Clemendot, F. Hutschka, J. Catal. 183 (1999) 107.
[59] G.H. Luo, X.Q. Wang, X.S. Wang, Chin. J. Catal. 19 (1) (1998) 53.
[60] H.H. Shan, C.Y. Li, C.H. Yang, H. Zhao, B.Y. Zhao, J.F. Zhang, Catal. Today 77 (2002) 117–126.
[61] A. Corma, C. Martinez, G. Ketley, G. Blair, Appl. Catal. A: Gen. 208 (2001) 135–152.